PROCEEDINGS OF SCIENCE

The plasma shock age, t, or the time elapsed after the shock front passed through the plasma, is estimated to be on the order of a few Myr for the NPS/Loop I; this places a strict lower limit to the age of the whole NPS/Loop I structure. We observe that NEI result in significantly higher temperature and lower emission measure than those currently derived under CIE assumption. Whereas the electron temperature is uniform at kT ~0.6 keV in the high-latitude NPS/Loop I region, about twice the temperature that is estimated in the state of CIE, the temperature changes from 0.3 keV to 0.6 keV in the low-latitude region. We discuss the implication of introducing NEI for the research in plasma states in astrophysical phenomena.

Discovery of non-equilibrium ionization plasma around the Fermi Bubble; new evidence of past activity of the Galactic center

Marino Yamamoto,[a,*] **Jun Kataoka**[a] **and Yoshiaki Sofue**[b]

[a] *Faculty of Science and Engineering, Waseda University, 3-4-1, Okubo, Shinjuku, Tokyo 169-8555, Japan*
[b] *Institute of Astronomy, The University of Tokyo, 2-21-2, Osawa, Mitaka-shi, Tokyo 181-0015, Japan*

E-mail: maricat@akane.waseda.jp

Fermi bubbles are giant gamma-ray structures toward the Galactic center (GC) with a symmetrical north–south extension perpendicular to the galactic plane. Such giant structures toward the GC are also observed at various wavelengths from radio to X-rays, such as WMAP haze, North Polar Spur (NPS), and most recently, eROSITA bubbles. We investigated the detailed plasma condition of the NPS/Loop I around Fermi bubble using archival *Suzaku* data. In the previous study, collisional ionization equilibrium (CIE) was assumed for the plasma state. However, we also assumed non-equilibrium ionization (NEI) to check the plasma condition in more detail. We found that most of the plasma in the NPS/Loop I favors the state of NEI that is characterized by the density-weighted ionization timescale of $n_e t \sim 10^{11-12}$ s cm^{-3}, and the electron number density $n_e \sim$ a few $\times 10^{-3}$ cm^{-3}.

7th Heidelberg International Symposium on High-Energy Gamma-Ray Astronomy (Gamma2022)
4-8 July 2022
Barcelona, Spain

*Speaker

1. Introduction

Large structures were observed in the direction of the galactic center (GC) at various wavelengths. An excess was observed in microwaves called WMAP[1], which was recently confirmed to exist on the Plank satellite[2]. The Fermi bubble observed in gamma rays also have a structure symmetrical to that of the galactic plane[3]. In contrast, the North Polar Spur (NPS) was discovered by the ROSAT all-sky survey (RASS) in X-rays to the northeast of the GC[4]. Multiple loop structures have been identified by X-ray and radio [5, 6], with the particularly bright and large northern structure being Loop I. These X-ray structures were remarkable only on the north side and asymmetric north–south when discovered, but the eROSITA satellite has discovered the north–south symmetric eROSITA bubble[7] in X-rays.

Although multi-wavelength observations have revealed large-scale structures in the GC direction, such as NPS/Loop I, the origin of these structures is still under debate. These structures were thought to be nearby supernova remnants (SNR) that recently appeared because of the observation of polarization and the north–south asymmetry of the structure when they were first discovered in radio waves and X-rays[5, 8]. However, after the discovery of the Fermi bubble, a north–south symmetric structure, the hypothesis that these structures are outflows from the GC a few Myr ago, came into the spotlight[9–11]. The eROSITA bubble, a recently discovered north-south symmetric structure, also supports this hypothesis.

Previous studies using X-ray spectral analysis assuming ionized equilibrium plasma have shown that the NPS/Loop I structure is hotter, with $kT \sim 0.3$ keV [12–14], than the temperature of a typical Galactic halo (GH), with $kT \sim 0.2$ keV [15]. In the scenario of GC production, these structures might have been produced over 10 Myr ago as a result of shock waves with velocity $v_{sh} \sim 300$km s^{-1} [16], stirring up the interstellar medium (ISM). It is not sure, however, for the plasma in NPS/Loop I to actually reach ionization equilibrium. Indeed, after a supernova explosion, ionization temperature T_z of the plasma takes a long time to catch up with electrons temperature T_e and protons temperature T_p, when analyzing SNR, the state of non-equilibrium ionization plasma (NEI) is assumed. In this study, we revisited the archival data of *Suzaku* under the assumption of the NEI state of the plasma as in SNR to investigate the origin of the large structure toward GC such as the NPS/Loop I.

2. Observation and Analysis

We used archived *Suzaku* X-ray Imaging Spectrometer (XIS) [17] data for our analysis. XIS is an X-ray CCD camera that covers an energy range of 0.2 – 12 keV characterized by its good energy resolution at low energy and low background; this is appropriate for diffuse gas analysis such as this study. The *Suzaku* satellite has four XISs: XIS0, 2, and 3 are front-illuminated (FI), and XIS1 is back-illuminated (BI). However, XIS2 was damaged in November 2006; therefore, data from three XISs were used in this analysis.

We analyzed 20 regions of bright emission in RASS as measured in the 0.75 keV (R34) band around the NPS/Loop I structure. Specifically, the brightest region NPS at low galactic latitude by Miller et al. [18], the eight regions N1-N8 across the Fermi bubble edge by Kataoka et al. [12], and slightly fainter emission ON8–16 and OFF4, 7 at high galactic latitude by Akita et al. [13]. The analysis regions are plotted in 0.75 keV image of RASS, as shown in Figure 1.

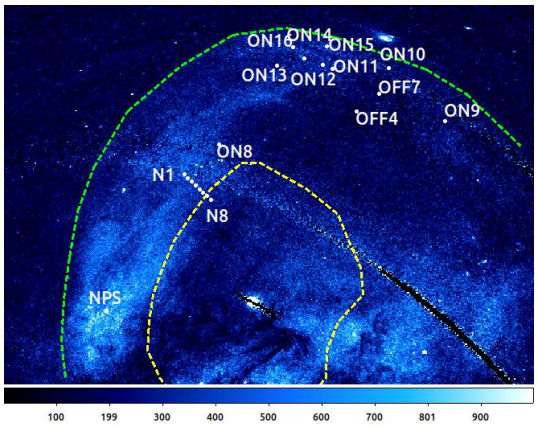

Figure 1: Observation region of the *Suzaku* XIS archival data shown on the *ROSAT* all–sky image of 0.75 keV. Yellow dashed line indicates the edge of the Fermi bubble [3], green dashed line indicates the edge of the eROSITA bubble, and white circle indicates the 17.8 arcmin field of view of the *Suzaku* XIS. The color bar is at the bottom of the figure, and the unit is 10^6counts s^{-1}.

We used `HEASOFT` version 6.27, `XSPEC` version 12.11.0, `xronos` version 6.0, and the calibration data set `CALDB` released on October 10 to perform data reduction for this analysis. We first used `xselect` to combine the screened data of each XIS0, 1 and 3 from 3×3 and 5×5, which are different observation modes. We then applied these criteria to the data using `xselect` based on the mkf file to perform data reduction: (1) remove data at the time of passing South Atlantic Anomaly (SAA) and 436 seconds later, as well as data for times when the solar wind proton flux is greater than $4.0 \times 10^8 \mathrm{cm}^{-2}\ \mathrm{s}^{-1}$ to mitigate the effect of solar wind charge exchange (SWCX) [15]; (2) use data with the rim of the earth (ELV) greater than 20° in the daytime and 5° in the night; (3) select data with cutoff rigidity (COR) greater than 6 GeV; and (4) remove data where the satellite pointing angle deviates more than 1.5 arcsec from the average. Furthermore, calibration sources, hot pixel, and flickering pixel were removed. To complete the image preparation, count rate correction was performed using `xisexpmapgen` [19], non-X-ray background (NXB) creation using `xisnxbgen` [20], and vignetting correction using `xissim` [19].

Before preparing the spectra, we removed the pointing sources detected by `XIMAGE` with a significance of more than 3σ because we wanted to analyze diffuse plasma of the NPS/Loop I in this study. We also created redistribution matrix files (RMFs) and auxillary response files (ARFs) assuming uniform radiation from a circle of radius 20 arcmin using `xisrmfgen` and `xissimarfgen` [19].

3. Results

We performed a spectral analysis for 0.6–7.0 keV of XIS0 and 3 (FI) and 0.4-5.0 keV of XIS1 (BI) using `XSPEC`. Based on previous studies [12, 13, 15], fitting was performed assuming that the plasma contained three components; (1) unabsorbed thermal emission of local hot bubble (LHB) and SWCX using the `apec` model with the plasma temperature and metal abundance fixed at $kT = 0.1$ keV and $Z = Z_\odot$, respectively, (2) absorbed thermal emission of GH and NPS/Loop I with the metal abundance fixed at $Z = 0.2Z_\odot$, and (3) absorbed non-thermal emission of cosmic X-ray

background (CXB) represented by single power law with the photon index fixed at $\Gamma = 1.41$. The neutral absorption column density $N_{H,Gal}$ was fixed at the full Galactic column value [21], and all of the normalization was set to free. Notably, for GH and NPS/Loop I plasma, previous studies only used the `apec` model assuming CIE, with statistically enough fitting results. However, in this study, we want to investigate the degree of NEI; therefore, we use both the `apec` model assuming CIE and the `nei` model assuming NEI. The `nei` model includes a parameter compared with the `apec` model called density-weighted timescale $n_e t$, that is the product of electron density n_e and shock age t and characterizes the degree of ionization equilibrium. If the density-weighted timescale is greater than $n_e t \sim 10^{12}$s cm^{-3}, it is considered a CIE plasma [22].

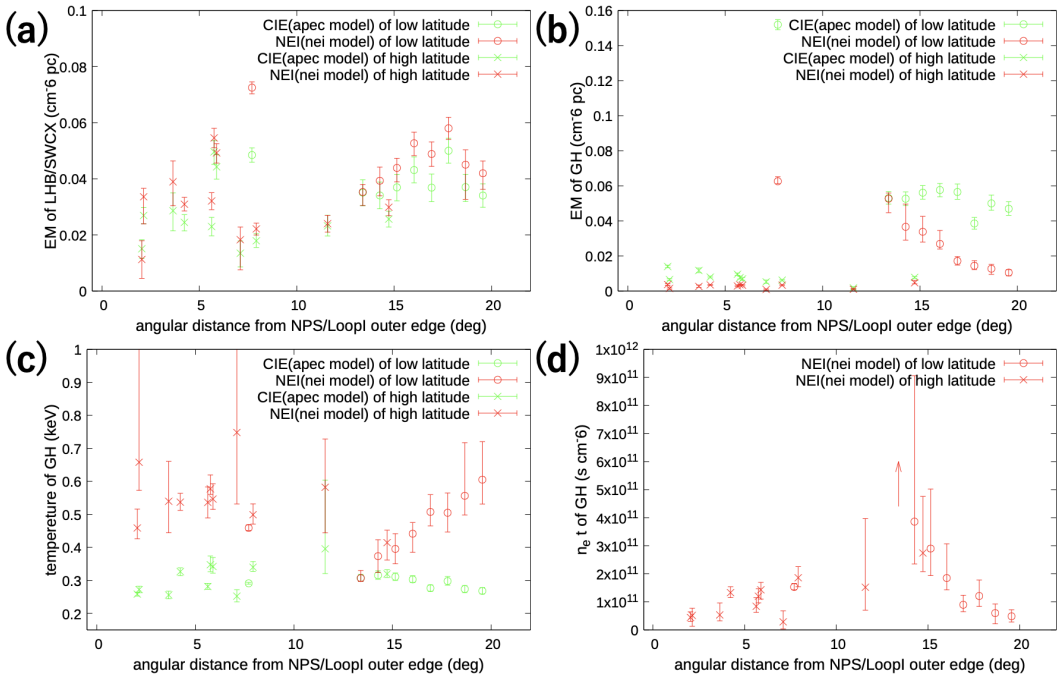

Figure 2: Comparison of results of spectral fitting toward NPS/Loop I region in the `apec` (CIE) and `nei` (NEI) models. In the horizontal axis, the angular distance from the northern edge of the eROSITA bubble that we defined (see, green dashed line in Fig.1) is plotted with the GC direction as positive.
(a) EM of the LHB/SWCX. (b) EM of the GH. (c) Electron temperature of the GH. (d) Density-weighted timescale of the GH.

The fitting results are shown in Fig.2. The emission measure (EM) was calculated using Eq.(1) of Stawarz et al. [23]. Furthermore, the temperature estimated by this fitting is the electron temperature. The NSP/Loop I component has different results for the assumption between the `apec` and `nei` model, whereas the LHB/SWCX component has almost the same results. For the plasma of the NPS/Loop I component, the NEI state is assumed to have higher temperatures and lower EM than those of the CIE state. Indeed, plasma temperature is $kT \sim 0.3$ keV in the CIE state, whereas it is ~ 0.6 keV assuming the NEI sate. The density-weighted timescale $n_e t$ is also $\sim 10^{11}$s cm^{-3}, suggesting that these plasma are in the NEI state close to the CIE. In particular, the aligned region of N1–N8, plotted in Fig.2 as low-latitude, shows gradually hotter, fainter emission and NEI as it comes closer to the GC. As the EM which is proportional to n_e decreases, the density-weighted

timescale $n_e t$ also decreases, thus the plasma becomes non-equilibrium.

As the reduced chi-squared χ^2/dof of the fitting results is ~ 1 for both the `apec` model and the `nei` model, the fitting is statistically appropriate, but the `nei` model does slightly better fitting. To confirm the advantage of the `nei` model, we performed the F-test, and in most regions, the P-value is less than 0.05; hence, the null hypothesis that the observation data are consistent with the fitting model when considering the 95% confidence interval, can be rejected. However, the `apec` model cannot be completely rejected from this result. The `apec` model can be regarded as the `nei` model where the density-weighted timescale is fixed at $n_e t \sim 10^{12-13}$s cm^{-3}.

4. Discussion

The electron density n_e can be calculated by assuming the scale length of the observed object and Eq.(1) of Stawarz et al. [23]. If the NPS/Loop I is assumed to be outflow near the GC at 8 kpc from the sun, the scale length is about 2 kpc, and the electron density is $n_e = (2-5)\times10^{-3}$cm^{-3} when calculated using the fitting results. This result is consistent with the $n_e \sim 3 \times 10^{-3}$cm^{-3} obtained in Kataoka et al. [12]. The explosion energy can be calculated as $E \simeq n_g \times kT \times V \sim 10^{54-55}$erg, where n_g denotes the gas density and $n_g \sim n_e$, and V denotes the total volume of the compressed gas number density, and the shock age, which represent the time elapsed since the shock wave passed, obtained from the density-weighted timescale $n_e t$ and electron density n_e is few Myr. This result is consistent with the outburst that occurred 10 Myr ago in GC [9, 10]. Alternatively, if the NPS/Loop I is the structure associated with nearby SNR at 100 pc from the sun, the scale length is about 50 pc, the electron density is $n_e \sim 2 \times 10^{-2}$cm^{-3}, explosion energy is $E \sim 10^{52}$erg, and shock age is 300 kyr according to the calculation using fitting results. This result is unnatural because the shock age is much longer than the typical SNR age. Therefore, we consider the NPS/Loop I structure to be outburst in GC.

When an explosion occurs in space, the shock wave generated by the explosion continues to heat the ISM. As the ISM is heated, the proton is hotter than the electron because of the $m_p/m_e \simeq 1836$, where m_p and m_e denotes the masses of proton and electron, and the proton and electron temperatures become non-equilibrium. Both the proton and electron follow a Maxwell distribution with self-collision. Then the proton transfers kinetic energy to the electron and reaches equilibrium in $t_{ep} \sim$ 1Myr when the electron density is $n_e = 3 \times 10^{-3}$cm^{-3} and the electron temperature is $kT_e = 0.3$ keV [24]. However, it takes $t_{CIE} \sim$ 10Myr for the ionization temperature of the plasma to reach equilibrium with the temperature of the electrons and protons (CIE), because density-weighted timescale need to be $n_e t \geq 10^{12}$s cm^{-3}.

However, since the analysis region in this study is sparse, a denser analysis using eROSITA and other data will provide new insights into large structure in the GC direction, such as the NPS/Loop I structure.

References

[1] Finkbeiner, D. P. 2004, ApJ, 614, 186. doi:10.1086/423482

[2] Planck Collaboration, Ade, P. A. R., Aghanim, N., et al. 2013, A&A, 554, A139. doi:10.1051/0004-6361/201220271

[3] Su, M., Slatyer, T. R., & Finkbeiner, D. P. 2010, ApJ, 724, 1044. doi:10.1088/0004-637X/724/2/1044

[4] Snowden, S. L., Freyberg, M. J., Plucinsky, P. P., et al. 1995, ApJ, 454, 643. doi:10.1086/176517

[5] Berkhuijsen, E. M., Haslam, C. G. T., & Salter, C. J. 1971, A&A, 14, 252

[6] Haslam, C. G. T., Salter, C. J., Stoffel, H., et al. 1982, A&AS, 47, 1

[7] Predehl, P., Andritschke, R., Arefiev, V., et al. 2021, A&A, 647, A1. doi:10.1051/0004-6361/202039313

[8] Bingham, R. G. 1967, MNRAS, 137, 157. doi:10.1093/mnras/137.2.157

[9] Sofue, Y. 1977, A&A, 60, 327

[10] Sofue, Y. 2000, ApJ, 540, 224. doi:10.1086/309297

[11] Bland-Hawthorn, J. & Cohen, M. 2003, ApJ, 582, 246. doi:10.1086/344573

[12] Kataoka, J., Tahara, M., Totani, T., et al. 2013, ApJ, 779, 57. doi:10.1088/0004-637X/779/1/57

[13] Akita, M., Kataoka, J., Arimoto, M., et al. 2018, ApJ, 862, 88. doi:10.3847/1538-4357/aacd08

[14] LaRocca, D. M., Kaaret, P., Kuntz, K. D., et al. 2020, ApJ, 904, 54. doi:10.3847/1538-4357/abbdfd

[15] Yoshino, T., Mitsuda, K., Yamasaki, N. Y., et al. 2009, PASJ, 61, 805. doi:10.1093/pasj/61.4.805

[16] Kataoka, J., Sofue, Y., Inoue, Y., et al. 2018, Galaxies, 6, 27. doi:10.3390/galaxies6010027

[17] Koyama, K., Tsunemi, H., Dotani, T., et al. 2007, PASJ, 59, 23. doi:10.1093/pasj/59.sp1.S23

[18] Miller, E. D., Tsunemi Hiroshi, Bautz, M. W., et al. 2008, PASJ, 60, S95. doi:10.1093/pasj/60.sp1.S95

[19] Ishisaki, Y., Maeda, Y., Fujimoto, R., et al. 2007, PASJ, 59, 113. doi:10.1093/pasj/59.sp1.S113

[20] Tawa, N., Hayashida, K., Nagai, M., et al. 2008, PASJ, 60, S11. doi:10.1093/pasj/60.sp1.S11

[21] Dickey, J. M. & Lockman, F. J. 1990, ARA&A, 28, 215. doi:10.1146/annurev.aa.28.090190.001243

[22] Smith, R. K. & Hughes, J. P. 2010, ApJ, 718, 583. doi:10.1088/0004-637X/718/1/583

[23] Stawarz, Ł., Tanaka, Y. T., Madejski, G., et al. 2013, ApJ, 766, 48. doi:10.1088/0004-637X/766/1/48

[24] Spitzer, L. 1962, Physics of Fully Ionized Gases, New York: Interscience (2nd edition), 1962